Fiber Bragg grating sensors with ultrahigh or ultralow temperature sensitivity

Zipei Song,[1] Mohan Wang, Patrick S. Salter, Tongyu Liu, Steve J. Elston, Martin J. Booth, Stephen M. Morris, and Julian A. J. Fells[2]

Department of Engineering Science, University of Oxford, Parks Road, Oxford, OX1 3PJ, UK

[1] *zipei.song@eng.ox.ac.uk*

[2] *julian.fells@eng.ox.ac.uk*

Abstract: Fiber Bragg grating (FBG) sensors have temperature sensitivities around +10 pm/°C. We fabricate an FBG with -55 pm/°C for discriminating temperature from other parameters and another stable to +/-12.5 pm over 17-45°C for temperature-independent measurements.

1. Introduction

Fiber Bragg grating (FBG) sensors are ubiquitous because they allow remote measurements of many physical parameters at multiple points, with high sensitivity and large dynamic range. However, a fundamental problem that has existed since their inception is that they are sensitive to both strain and temperature simultaneously. The thermal shift in Bragg wavelength arises from thermal expansion and the dependence of the refractive index on temperature. In contrast, the strain response arises from both the physical extension and photoelastic effect [1]. For a typical silica FBG sensor at 1550 nm, the strain response is approximately 1.2 pm/$\mu\varepsilon$ [2] and the thermal response is approximately 11.3 pm/°C [3]. However, because of the dual sensitivity of FBG sensors to temperature and strain, it is impossible to monitor either of them with a single measurement of the Bragg wavelength. Discrimination between temperature and strain has therefore attracted broad attention and continuous attempts have been made over the last four decades.

Fiber Bragg gratings can be stabilized by putting them in a package that relieves the strain as the temperature increase [4]. However, the package prevents the FBG from being used as a strain sensor. One way to achieve strain and temperature discrimination would be to have two FBGs that have different temperature or different strain coefficients. Tapered fibers have been used to get different strain coefficients [5] but suffer from poor mechanical strength. Interrogating at two different wavelengths [6] or two different polarizations [7] to get different temperature coefficients has been tried, but the differences in sensitivity are small. One solution proposed is to use liquids that have a negative temperature coefficient. Kim *et al.* etched the cladding away and dipped the end in a liquid [8], but this is not practical for embedded sensors; There have been a number of theoretical papers proposing custom-made fibers filled with liquid [9, 10], but so far there have been no practical demonstrations.

There have been a number of reports of microstructured fiber with an array of holes in the cross-section that have been filled with liquid. Liquid, compared with fused silica that standard fibers are made of, presents a significant and negative thermo-optic coefficient dn/dT. Naeem *et al.* were able to achieve a modest change in temperature sensitivity using methanol-filled holes [11]. Huy *et al.* showed plots with flattened temperature response but did not show spectra for the filled fibers [12]. When the microstructure is filled with the liquid, it is no longer microstructured as the liquid refractive index is close to the cladding refractive index. Our analysis of this structure shows that it will be multimoded and therefore not have a single reflection peak needed for accurate sensing. In this work, we fabricate FBGs with intrinsically modified temperature coefficients to enable decoupling of strain and temperature sensitivity, while maintaining good spectral properties.

2. Design Concept

An FBG sensor device with a very different thermal response is needed in order to discriminate the temperature response from the strain response. The Bragg wavelength shift $\Delta\lambda_B$ with temperature and strain is given by [1]:

$$\frac{\Delta\lambda_B}{\lambda_B} = \left(1 - \left(\frac{n_{eff}^2}{2}\right)[P_{12} - \nu\,(P_{11} + P_{12})]\right)\varepsilon + (\alpha + \xi)\Delta T \tag{1}$$

where ε is strain, ΔT is the temperature change, P_ij are the Pockel's coefficients of the stress-optic tensor, ν is Poisson's ratio, α is the thermal expansion coefficient and ξ is the thermal response of the fiber. Although α

mainly depends on the fiber material, ξ is dependent on the effective refractive index n_{eff} of the FBG, given by $\xi = \frac{1}{n_{eff}} \frac{dn_{eff}}{dT}$. In an FBG ξ is approximately proportional to the thermo-optic coefficient of the fiber material (7.97×10^{-6} C^{-1} for fused silica [13]). The Bragg wavelength shift of a silica step-index fiber due to an increase in temperature is always positive across all temperature ranges. In order to improve the thermal response, we create custom microchannels in the fiber and fill them with a high magnitude $\frac{dn}{dT}$ material to achieve the desired ξ. Refractive index liquids from CARGILLE LABS were selected for a much larger magnitude thermo-optic coefficient of -395×10^{-6} C^{-1} [14] than that of fused silica. Furthermore, a set of refractive index oils can be found with refractive indices between 1.420 to 1.460 at 1550 nm at room temperature [14] to match the refractive index of fused silica.

The cross-section of the FBG device was designed to have four channels as shown in Fig. 1(a). An FBG is written within the core and microchannels filled with refractive index oil are in the cladding in close proximity to the fiber core without touching it.

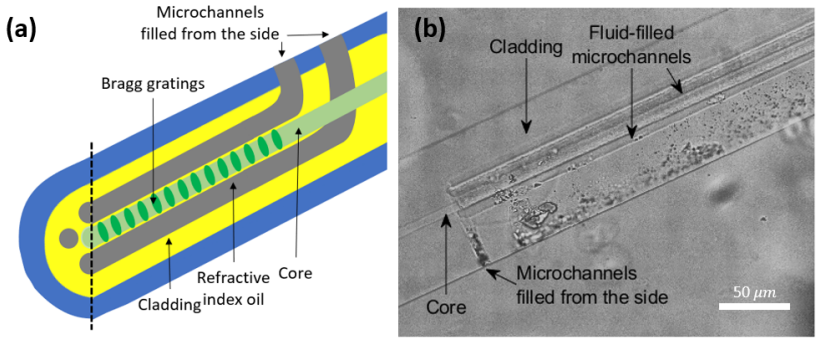

Fig. 1: (a) Sketch of the device (not to scale) in a section of fiber. (b) A microscope image of a micro-structured FBG device near one end of the microchannels.

3. Method of fabrication

The microchannels are formed by laser writing in the fiber followed by a selective etch to remove the material in the exposed regions. A regenerative femtosecond laser system (Light Conversion Pharos SP-06-1000-PP) was used to fabricate the necessary pattern inside the fiber. For fabrication, a second harmonic generation wavelength of 515 nm was used with a pulse duration of 170 fs. A half-waveplate in conjunction with a polarizer was used to control the pulse energy between 10 and 300 nJ. A spatial light modulator (SLM) (Hamamatsu X10468) was used to compensate for the aberration generated in the optical path of the whole system. The sample fiber was taped onto a microscope slide and placed on a motion stage (x, y: Aerotech ABL10100L and z: ANT95-3-V) to provide different focus positions for the laser. The objective used had a $\times$20 magnification and numerical aperture of 0.5. A second-order FBG was written in a single-mode fused silica fiber (SMF28e+) by scanning the laser focus along the center of the fiber core by setting the laser pulse repetition rate and the scanning speed appropriately. The FBG was written inside the fiber core, with a pulse energy of 0.15 μJ and a repetition rate of 100 Hz controlled by a pulse picker. The writing speed was 0.1071 mm/s so that after the strain induced by the fiber mounting was relieved, the Bragg wavelength was approximately 1550 nm. The microchannels were written and brought to the fiber surface, without going through the fiber core, with a slightly higher pulse energy 0.26 μJ at a repetition rate of 250 kHz at a speed of 0.1 mm/s, with polarization perpendicular to the writing direction. They are written alongside the core, with access points to the fiber surface to enable filling. The device was fabricated without immersion oil, thus aberration correction for the fiber surface in the air was required [15]. The FBG is 3 mm long and the channels are 3 mm long as well with access channels every 1.5 mm to achieve roughly uniform etching along the fiber length. The device was placed in a KOH solution for etching to preferentially remove the laser-exposed regions. Finally, the etched microchannels were filled with refractive index oil by capillary action.

4. A high thermal sensitivity FBG device

One aim is to fabricate a high thermal sensitivity FBG device that will be used for temperature and strain discrimination. The highest sensitivity would be obtained with the core completely surrounded by liquid, but this would be mechanically unstable. Therefore, some connections are left in between the microchannels as shown in Fig. 2 (a). There are 4 microchannels along the core, positioned symmetrically within the fiber cross-section. Each of the four channels is about 7 μm wide and 10 μm long leaving approximately 0.5 μm gap between one other. The

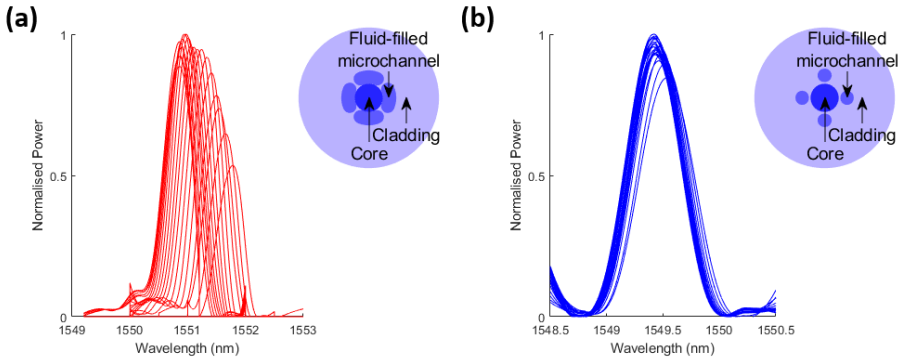

Fig. 2: The reflection spectrum at different temperatures (a) from 4°C to 40°C of a high thermal sensitivity FBG device with the cross-section profile, (b) from 5°C to 49°C of a compensated thermal sensitivity FBG device with the cross-section profiles

FBG with microchannels was fabricated with the laser parameters stated above and was then placed in 8 mol/L KOH solution for approximately 13 hours at 60°C, using a water bath on a hot plate. A relatively high refractive index for the oil was chosen to be 1.440 at 1550 nm so that the operating temperature is around room temperature.

At the temperature range of 4°C to 20°C the thermal sensitivity $\frac{\Delta\lambda_B}{\Delta T}$ was measured to be approximately -42 pm/°C, while between 4°C and 50°C the thermal sensitivity was measured to be around -25 pm/°C. The Bragg wavelengths of a conventional FBG fabricated in the same fiber are also shown, giving a thermal sensitivity of 10 pm/°C. The peak power reflectivity R_{max} is given by $R_{max} = \tanh^2(\kappa L_g)$ where κ is the coupling coefficient and L is the length of Bragg grating. The peak reflectivity at 24°C drops to 0.53 of that at 40°C. At a lower temperature, the oil refractive index is closer to the core index, so the mode expands further into the microchannel region thus the coupling coefficient is lower. As a result, we expect a high thermal response but a lower peak reflection. As temperature increases, the coupling coefficient gradually decreases, thus the thermal response decreases while the peak reflection increases. The fullwidth half maximum (FWHM) for the measured spectrum at different temperatures is approximately uniform at 0.5 nm.

5. A compensated thermal sensitivity FBG device

An FBG sensor device with a compensated thermal response has been fabricated that could be used for temperature-independent strain sensing with individual FBGs. The non-linear thermal response with temperature has a turning point where the thermal response crosses zero. In order to keep a low thermal response near the turning point we reduced the fluid proportion in the evanescent field by moving the microchannels further away from the core, as shown in Fig. 2 (b). The four channels are circular in shape with a diameter of approximately 7 μm leaving a larger gap of 1 μm away from the core to allow for some over-etch. The FBG was written with the same parameters as the high sensitivity device. The microchannels were fabricated with a slightly higher pulse energy of 0.290 μJ to overcome the aberration caused by the asymmetric fiber top surface when the focal position is further away from the center. The fiber was then placed in 8 mol/L KOH solution and etched for approximately 15 hours at 60 °C using a waterbath on a hotplate.

The oil refractive index was chosen to be 1.44 at 1550 nm so that the device is optimized for room temperature with zero sensitivity centered at approximately 30°C. The measured reflection spectrum is plotted in Fig. 2 (b) and shows an approximate bandwidth of 0.5 nm depending slightly on temperature. The relative intensity within the range of 17°C to 45°C varies within only 6.9%, indicating that this device is insensitive to temperature in terms of both Bragg wavelength and power reflectivity. The Bragg wavelengths are shown in Fig. 3 which shows a compensated thermal sensitivity of ±12.5 pm on average within a room temperature range of 17°C to 45°C.

6. Conclusion

To conclude, we have demonstrated FBG devices with micro-engineered thermal sensitivities. The devices are fabricated by laser inscription followed by chemical etching to allow liquid refractive index oil to be filled into the cladding of the standard single-mode fiber. A device with a large thermal response has been fabricated and measured to have a near second-order thermal sensitivity of up to -55 pm/°C near 4°C and an average thermal response of -25 pm/°C over the range of 4°C to 50°C. The device gives an extraordinarily large thermal sensitivity over 5 times that of conventional silica FBGs, potentially allowing strain-temperature discrimination. Another device has shown an exceptionally low thermal variation of ±12.5 pm over a temperature range of 17°C to 45°C.

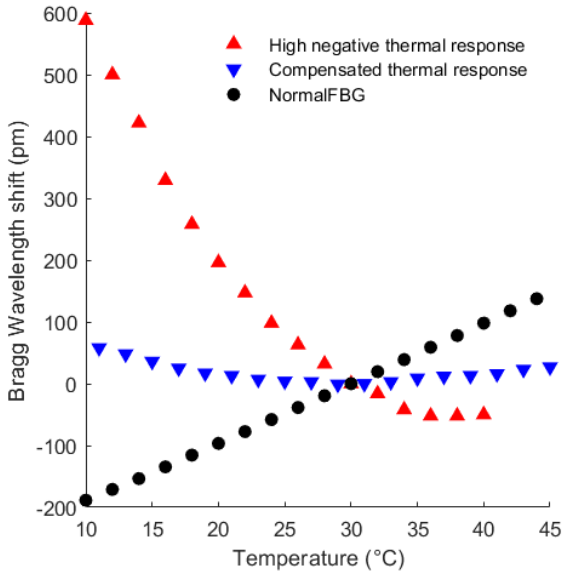

Fig. 3: Plot of measured reflected Bragg wavelength against temperature for a high negative thermal response FBG device, a compensated thermal response FBG device, and a conventional FBG.

This sensitivity is an order of magnitude less than conventional FBGs, potentially allowing temperature-insensitive strain measurements without additional compensation.

References

1. A. D. Kersey, M. A. Davis, H. J. Patrick, M. LeBlanc, K. P. Koo, C. G. Askins, M. A. Putnam, and E. J. Friebele, "Fiber grating sensors," J. lightwave technology **15**, 1442–1463 (1997).
2. Y. J. Rao, A. B. L. Ribeiro, D. A. Jackson, L. Zhang, and I. Bennion, "Combined spatial-and time-division-multiplexing scheme for fiber grating sensors with drift-compensated phase-sensitive detection," Opt. letters **20**, 2149–2151 (1995).
3. B.-O. Guan, H.-Y. Tam, X.-M. Tao, and X.-Y. Dong, "Simultaneous strain and temperature measurement using a superstructure fiber Bragg grating," IEEE Photonics Technol. Lett. **12**, 675–677 (2000).
4. Y. Huang, J. Li, G. Kai, S. Yuan, and X. Dong, "Temperature compensation package for fiber Bragg gratings," Microw. Opt. Technol. Lett. **39**, 70–72 (2003).
5. H. F. Lima, P. F. Antunes, J. de Lemos Pinto, and R. N. Nogueira, "Simultaneous measurement of strain and temperature with a single fiber Bragg grating written in a tapered optical fiber," IEEE Sensors J. **10**, 269–273 (2009).
6. M. G. Xu, J.-L. Archambault, L. Reekie, and J. P. Dakin, "Discrimination between strain and temperature effects using dual-wavelength fibre grating sensors," Electron. letters **30**, 1085–1087 (1994).
7. A. K. Singh, S. Berggren, Y. Zhu, M. Han, and H. Huang, "Simultaneous strain and temperature measurement using a single fiber Bragg grating embedded in a composite laminate," Smart Mater. Struct. **26**, 115025 (2017).
8. K. T. Kim, I. S. Kim, C.-H. Lee, and J. Lee, "A temperature-insensitive cladding-etched fiber Bragg grating using a liquid mixture with a negative thermo-optic coefficient," Sensors **12**, 7886–7892 (2012).
9. N. Mothe, D. Pagnoux, M. C. P. Huy, V. Dewinter, G. Laffont, and P. Ferdinand, "Thermal wavelength stabilization of Bragg gratings photowritten in hole-filled microstructured optical fibers," Opt. Express **16**, 19018–19033 (2008).
10. W. Man, C. Zhang, J. Huang, and Q. He, "Optimization design of temperature-insensitive Bragg gratings inscribed in ethanol-filled photonic crystal fibers," Opt. Eng. **58**, 116101 (2019).
11. K. Naeem and Y. Chung, "Strain and temperature discrimination using PCF Bragg-gratings filled with different liquids," in *2014 OECC and Australian Conference on Optical Fibre Technology,* (IEEE, 2014), pp. 795–796.
12. M. C. P. Huy, G. Laffont, V. Dewynter, P. Ferdinand, D. Pagnoux, B. Dussardier, and W. Blanc, "Passive temperature-compensating technique for microstructured fiber Bragg gratings," IEEE Sensors J. **8**, 1073–1078 (2008).
13. D. B. Leviton and B. J. Frey, "Temperature-dependent absolute refractive index measurements of synthetic fused silica," in *Optomechanical Technologies for Astronomy,* vol. 6273 (International Society for Optics and Photonics, 2006), p. 62732K.
14. CARGILLE LABS, "Refractive-Index-Liquid-Series-AA-n-1.4400-at-589.3-nm-and-25°C," Tech. rep. (2018).
15. P. S. Salter, M. J. Woolley, S. M. Morris, M. J. Booth, and J. A. J. Fells, "Femtosecond fiber Bragg grating fabrication with adaptive optics aberration compensation," Opt. letters **43**, 5993–5996 (2018).